

See discussions, stats, and author profiles for this publication at:  
<https://www.researchgate.net/publication/231397290>

# Optical Probing of Single Molecules of Terrylene in a Shpol'kii Matrix: A Two-State Single-Molecule Switch

ARTICLE in THE JOURNAL OF PHYSICAL CHEMISTRY · JULY 1994

Impact Factor: 2.78 · DOI: 10.1021/j100081a025

CITATIONS

118

READS

8

6 AUTHORS, INCLUDING:



**William Esco Moerner**

Stanford University

455 PUBLICATIONS 19,569 CITATIONS

SEE PROFILE



**Taras Plakhotnik**

University of Queensland

89 PUBLICATIONS 1,699 CITATIONS

SEE PROFILE



**Viktor Palm**

University of Tartu

54 PUBLICATIONS 472 CITATIONS

SEE PROFILE



**Urs P. Wild**

ETH Zurich

343 PUBLICATIONS 6,207 CITATIONS

SEE PROFILE

# Optical Probing of Single Molecules of Terrylene in a Shpol'skii Matrix: A Two-State Single-Molecule Switch

W. E. Moerner,<sup>\*,†</sup> Taras Plakhotnik,<sup>‡</sup> Thomas Irngartinger, Mauro Croci, Victor Palm,<sup>§</sup> and Urs P. Wild

Laboratory of Physical Chemistry, Swiss Federal Institute of Technology,  
ETH Zentrum, CH-8092, Zürich, Switzerland

Received: March 2, 1994; In Final Form: April 25, 1994\*

We report fluorescence excitation spectra of individual impurity molecules in a new system: terrylene in a Shpol'skii matrix of hexadecane. Studies of optical incoherent saturation, fluorescence microscope images, and resonance frequency changes are reported for the 0–0 electronic transition at 1.7 K. For four stable molecules, the low-power optical line width at 1.7 K is  $40 \pm 2$  MHz full width at half-maximum, the saturation intensity is near  $1 \text{ W/cm}^2$ , and the peak detected count rate can reach 11 000 counts per second. Most single molecules either are stable or require many minutes of irradiation before the resonance frequency changes suddenly, but some show spectral changes on a time scale of seconds. Since higher laser power increases the average rate of frequency shifts, this effect represents a light-driven change in the local environment analogous to nonphotochemical hole-burning in large ensembles. Several two-state molecules have been observed, and a preliminary characterization of this light-driven "molecular switch" has been completed. Multistate behavior also occurs. This work demonstrates that Shpol'skii matrices should provide fertile ground for the generation of a large number of new materials in which single-molecule spectra can be obtained.

## Introduction

The field of optical detection and spectroscopy of single molecules continues to show promise as a method of studying the properties of the local "nanoenvironment" of isolated impurity molecules in solids where ensemble averaging has been removed.<sup>1</sup> In the important model system composed of pentacene doped into crystalline *p*-terphenyl, fascinating effects such as spectral diffusion,<sup>2</sup> perturbations of photophysical parameters,<sup>3</sup> electric field,<sup>4</sup> and pressure<sup>5</sup> shifts, photon antibunching,<sup>6</sup> polarization effects,<sup>7</sup> and single-molecular-spin magnetic resonance<sup>8,9</sup> have been reported. The extension of single-molecule spectroscopy (SMS) to polymeric hosts has been reported for perylene in poly(ethylene) (PE)<sup>10</sup> and for terrylene in PE,<sup>11</sup> which has allowed preliminary study of many new physical effects arising from disorder such as nonphotochemical hole-burning<sup>12</sup> and two-level-system dynamics.<sup>13,14</sup>

In the past, only these three systems have allowed the recording of detailed high-resolution single-molecule spectra, partly because the requirements for narrow absorption features in SMS are rather restrictive:<sup>15</sup> high peak absorption cross section, weak or absent bottlenecks in the optical pumping cycle, large fluorescence quantum yield, a strong zero-phonon component in the lowest electronic transition, and weak or absent spectral hole-burning. To allow further expansion of the field, new materials which allow SMS are required.

In this paper, we report SMS for a new materials system, terrylene in the Shpol'skii matrix<sup>16</sup> hexadecane. As is well-known, Shpol'skii matrices are polycrystalline host materials formed by quenching of the lower *n*-alkanes to low temperatures to provide host matrices for a wide variety of impurity molecules.<sup>17</sup> The low-power limiting line width and the saturation behavior of a selection of stable single molecules are presented, and the minimum line width is in good agreement with the lifetime-limited value. Compared to those for the pentacene in *p*-terphenyl system,

the maximum emission rates from terrylene are larger by almost a factor of 5, and the saturation intensity is as much as 2 orders of magnitude higher. With the resulting large emission rates, high-quality three-dimensional fluorescence microscopy images can be obtained (intensity as a function of *x*, *y*, and excitation frequency).

Interestingly, upon extended irradiation by the pumping laser, the resonance frequency of some terrylene molecules changes, and evidence is presented from several techniques that this is a light-driven process rather than spontaneous spectral diffusion. Moreover, some terrylene molecules seem to have two stable resonance frequencies spaced by approximately 150 MHz, suggesting that such terylenes are coupled to exactly one two-level system in the matrix, surprisingly similar to a previous report for terrylene in PE.<sup>14</sup> Because light can be used to change the state (resonance frequency) of the single molecule, such centers can be regarded as a light-driven "molecular switch". Results from a multistate molecule (five resonance frequencies) are also presented. Since many alkane hosts form polycrystalline Shpol'skii matrices with multiple sites for impurity molecules of various sizes,<sup>17</sup> the terrylene in a hexadecane system is expected to be a model for a large new class of materials which should easily show single-molecule spectra. A preliminary report of this work has already appeared.<sup>18</sup>

## Experimental Section

Samples were prepared by dissolving a tiny speck of solid terrylene in hexadecane at room temperature to form a very light pink fluorescent mixture. With the measured optical density of this solution and an extinction coefficient of  $79\,400 \text{ L/mol}\cdot\text{cm}$ ,<sup>19</sup> the concentration was determined to be  $4.7 \times 10^{-7} \text{ mol/L}$ . The mixture was quenched to low temperature in three different sample geometries to form the Shpol'skii matrix (see below). All measurements were performed in pumped superfluid helium at  $1.7 \pm 0.1 \text{ K}$ .

Two sources of hexadecane were used: (i) a bottle several years old (Fluka, purum) which may have contained an unknown amount of water, and (ii) anhydrous hexadecane (Aldrich) with less than 0.005% water. No significant difference in the behavior

<sup>†</sup> Permanent address: IBM Research Division, Almaden Research Center, San Jose, CA.

<sup>‡</sup> Permanent address: Institute of Spectroscopy, Troitsk, Moscow Region, Russia.

<sup>§</sup> Permanent address: Inst. of Physics, Estonian Acad. Sci., Tartu, Estonia.

\* Abstract published in *Advance ACS Abstracts*, June 15, 1994.

of the two types of sample, so it is unlikely that hydrogen bonds are responsible for the time-dependent changes in resonance frequency described below.

### Fluorescence Excitation of a Sample with an Optical Fiber.

The optical setup for acquisition of fluorescence excitation spectra with a Rhodamine 6G single-frequency tunable dye laser was similar to that previously described,<sup>20</sup> with a few exceptions. The single-frequency pumping radiation was brought into the optical cryostat with a polarization-preserving optical fiber. A drop of the doped hexadecane solution was placed between the cleaved end of the fiber and a glass cover slip 130  $\mu\text{m}$  thick. In this manner, a thin sample some micrometers in thickness was probed by the laser beam emerging from the end of the fiber. To estimate the (free-space) probing light intensity, the optimum launch spot size of 3  $\mu\text{m}$  for the fiber was taken as the diameter of the pumping light beam. The emitted fluorescence transmitted through the glass plate was collected with a paraboloidal mirror and directed out of the cryostat. Rayleigh-scattered pump radiation was blocked by three Schott RG610 glass filters, and the long-wavelength-shifted fluorescence was detected by a GaAs photomultiplier and photon counting electronics as usual. In this manner, the fluorescence excitation spectrum was recorded as a function of the wavelength of the probing laser with 3 MHz resolution. The frequency scale was carefully calibrated using 100 MHz phase modulation side bands produced by an electrooptic modulator driven by a precision rf frequency synthesizer.

For low-resolution scans of the fluorescence excitation spectrum of the entire inhomogeneous line, the thick and thin etalons were removed from the laser and the wavelength was scanned using the birefringent filter. In this configuration, the laser line width was approximately 20 GHz. The sample for the low-resolution scans was made by trapping a small amount of the doped solution between two glass cover slips by capillary action and quenching this sample into liquid helium. The laser illuminated a spot of diameter approximately 1 cm for the low-resolution spectra.

**Fluorescence Imaging Microscopy.** In the "classical" single-molecule setup of the previous section, only a single (diffraction-limited) spatial volume of the sample is studied at a time. Recently, a high-sensitivity fluorescence microscope was developed<sup>21</sup> which allows recording of the emission at 1.7 K from a sample about 100  $\mu\text{m} \times 100 \mu\text{m}$  in size with a spatial resolution of  $\approx 3 \mu\text{m}$ . The microscope is based on a fast-scan, intensified two-dimensional multialkali cathode-vidicon camera (Hamamatsu) connected to a DataCube parallel image processor which can be run in a "high-sensitivity photon-counting" mode or in an "analog" mode. We have improved the collection efficiency of the original microscope by the addition of a microscope objective with numerical aperture 0.85 located in the superfluid helium approximately 300  $\mu\text{m}$  from the surface of the sample.

The sample for the microscopy measurements was prepared by spin-coating the doped hexadecane solution directly onto a glass cover slip. While this method does not form a layer of perfectly uniform thickness due to the liquid state of hexadecane at room temperature, the viscosity of the solution was sufficiently high that upon quenching into the precooled cryostat, a sample with acceptable optical quality was easily formed. A 100  $\mu\text{m}$  diameter aperture placed before the cover slip served to define the area which was imaged on the two-dimensional detector, and several long-pass filters were used to block the pump radiation as usual.

**Fast Fluorescence Excitation Scans for Time-Dependent Studies.** Since some terrylene single molecules showed resonance frequency changes on the second to minute time scale, a special fast-scan setup was used to record fluorescence excitation spectra from a fixed probing volume at scan speeds near the maximum available from the laser. This method<sup>2</sup> allows detailed information about the actual resonance frequencies visited by the single molecules to be recorded, in contrast to the correlation method<sup>14</sup>

which utilizes a fixed laser frequency but acquires dynamical information on a shorter time scale.

The ring dye laser and a 150 MHz free spectral range external confocal cavity, actively locked to a polarization-stabilized HeNe Laser (Newport NL1) for monitoring the laser drifts, have been described elsewhere.<sup>5</sup> The optical arrangement utilized a lens in the superfluid helium for focusing the pump radiation (adjustable in position by means of an electromagnet) and a paraboloid for the collection of the fluorescence emission as described earlier.<sup>20</sup> For purposes of estimating the laser intensity, we assume the focal spot size is similar to previous work (5  $\mu\text{m}$  FWHM).<sup>20</sup> One drop of the doped hexadecane solution was carefully put on a LiF plate and then covered with a glass cover slip held in place by capillary action. The plate was then placed at the joint focus of the focusing lens and the collection paraboloid. The sample was then quenched in the cryostat precooled with liquid nitrogen.

The laser frequency was scanned continuously up and down using a voltage ramp stored in the buffer of a digital-to-analog converter (IOtech DAC488). The fluorescence emission was detected by a GaAs photomultiplier as usual with long-pass filters to block the pump radiation. The discriminator output pulses from the photomultiplier were counted in a 24-bit home-built binary counter. A second counter registered the laser transmission signal through the stabilized cavity to provide a correction signal for long-term laser drift. To transfer the results to the controlling workstation, a digital input/output device (IOtech, Digital488/30) with buffering capability was used to avoid data losses during fast scans. The system allows the recording of sequential continuous frequency scans for hours, with reading times per point ranging from seconds down to a few milliseconds. A more detailed description of this setup will be published elsewhere.

### Photophysics of the Terrylene Molecule

For future reference, some photophysical parameters for terrylene which have been deduced from our data will be presented here. The (low temperature) peak absorption cross section  $\sigma_{\text{pk}}$  is a crucial quantity appearing in all calculations of the signal-to-noise ratio for a single molecule.<sup>1</sup> It can be estimated with knowledge of the integrated absorption coefficient and the (low temperature) homogeneous line width for the transition,  $\Delta\nu_{\text{H}}$ , by using<sup>15</sup>

$$\sigma_{\text{pk}} = \frac{2c}{\pi \Delta\nu_{\text{H}}} \left( \frac{\tilde{S}}{N_{\text{tot}}} \right) \quad (1)$$

where  $c$  is the velocity of light,  $\Delta\nu_{\text{H}}$  is the homogeneous line width full width at half-maximum (FWHM) in hertz, and  $N_{\text{tot}}$  is the number density of centers which produces the integrated absorption  $\tilde{S}$ . Only the contribution to  $\tilde{S}$  from the zero-phonon line (ZPL) is relevant, so  $\tilde{S}$  can be estimated from a room temperature measurement of the absorption coefficient of a solution with density  $N_{\text{tot}}$  using the expression

$$\tilde{S} = 3C_{\text{FC}} \int \alpha(\tilde{\nu}) d\tilde{\nu} \quad (2)$$

where  $\alpha$  is the absorption coefficient per unit length, the integral is performed over the entire  $S_1 \leftarrow S_0$  transition, and  $C_{\text{FC}}$  is the (low temperature) Franck-Condon factor expressing the fraction of the integrated absorption in the ZPL. The factor of 3 is included because we are interested in the microscopic cross section appropriate for a polarized laser beam with polarization along the molecular dipole moment, while the room temperature absorption measurement is an orientational average over all possible orientations of the molecules.  $C_{\text{FC}}$  was estimated to be 0.40 from a published low-temperature fluorescence emission spectrum of terrylene in PE.<sup>13,22</sup> From the measured  $\Delta\nu_{\text{H}}$  of 40 MHz (see the next section) and a room temperature absorption spectrum of the doped hexadecane,  $\sigma_{\text{pk}} \approx 2.2 \times 10^{-10} \text{ cm}^2$ . This

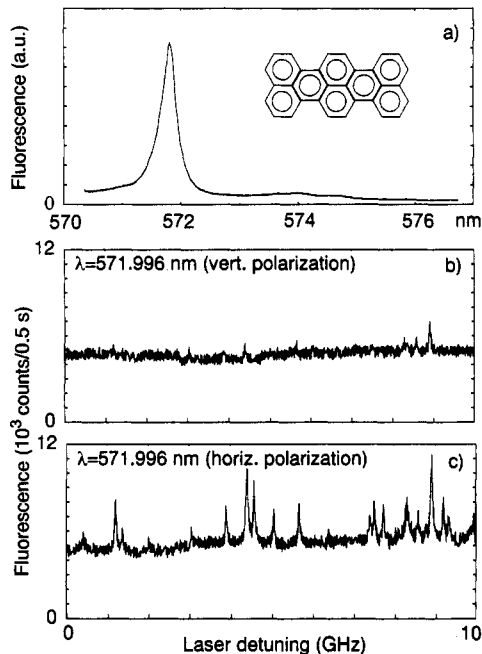


**Figure 1.** Excitation spectra of terrylene in hexadecane at 1.7 K. (a) Low-resolution scan of a sample between glass plates showing the dominant site origin at 571.9 nm. Inset: structure of terrylene. (b) High-resolution scan over 10 GHz at 571.996 nm of a small volume of solid at the end of an optical fiber, vertical polarization. (c) Scan of the same spectral range as in part b, but with the orthogonal polarization. Scan time for parts b and c, 4 min. Scanning intensity 1.2 W/cm<sup>2</sup>.

is a very large cross section which is approximately 1 order of magnitude larger than for pentacene,<sup>1</sup> and it means that the effective area terrylene presents to incoming photons is more than 10 000 times as large as the area of the molecule itself.

An expression similar to eq 1 can be used to compute the  $A$  coefficient or radiative rate for the transition,

$$A_{21} = \frac{8\pi c}{(\lambda_0/n)^2 N_{\text{tot}}} \int \alpha(\tilde{\nu}) d\tilde{\nu} = 1/\tau_{\text{rad}} \quad (3)$$

where  $\lambda_0$  is the free-space wavelength and  $n = 1.434$  is the refractive index. For terrylene,  $A_{21} = 1.8 \times 10^8 \text{ s}^{-1}$ , and from a fluorescence emission lifetime measured for terrylene in PE of  $T_1 = 3.78 \pm 0.03 \text{ ns}$ ,<sup>24</sup> the fluorescence quantum yield  $\Phi_F = T_1/\tau_{\text{rad}} = 0.69$ .

## Results and Discussion

**Basic Characteristics of the Single-Molecule Spectra.** Figure 1a shows the low-resolution fluorescence excitation spectrum of a polycrystalline sample of terrylene (structure, see inset) in hexadecane over a large wavelength range at 2 K. Only one strong site origin near 571.9 nm is observed, with two additional weak origins near 574.0 and 574.7 nm. (It is possible that additional origins lie to shorter wavelengths than those shown, beyond the scan range of the laser.) The 0.3 nm FWHM width of the zero-phonon line (ZPL) is comparable to other Shpol'skii matrix systems (for example, 0.4 nm FWHM for perylene in *n*-hexane at 5 K).<sup>17</sup> The crystal structure of hexadecane is triclinic<sup>25</sup> with unit cell dimensions  $a = 4.29 \text{ \AA}$ ,  $b = 4.81 \text{ \AA}$ ,  $c = 20.87 \text{ \AA}$  and angles  $\alpha = 91.9^\circ$ ,  $\beta = 80.5^\circ$ , and  $\gamma = 106.9^\circ$ . Since terrylene/hexadecane is a new Shpol'skii system, the actual packing in the unit cell is unknown at present. One might expect that the large value of  $c$  allows the long axis of terrylene (estimated skeletal dimension  $4.8 \text{ \AA} \times 8.4 \text{ \AA}$ )<sup>26</sup> to easily fit along the  $c$ -axis in the crystal. (An attempt to form a Shpol'skii system with the terrylene/*n*-octane pair produced almost no dissolution of the terrylene and no low-temperature ZPL origins.)

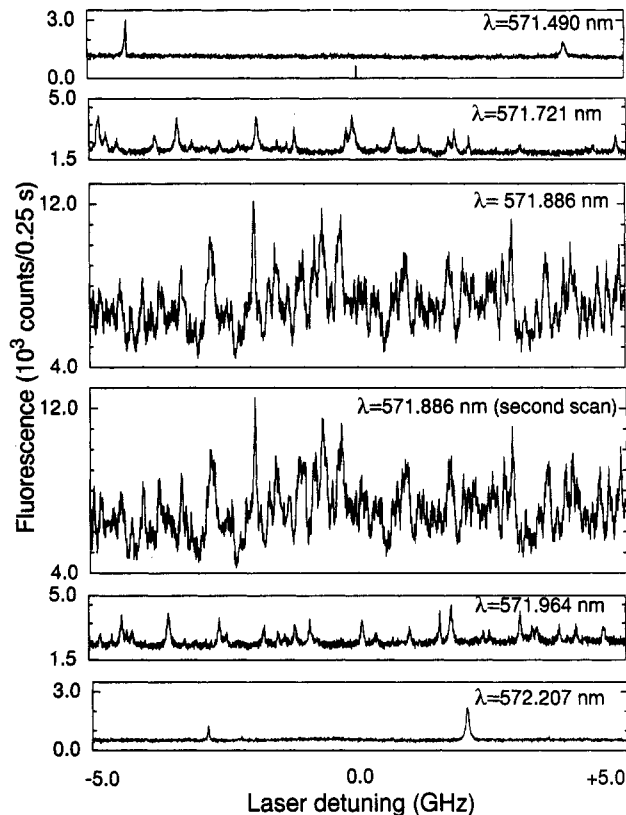


**Figure 2.** High-resolution excitation spectra at several positions relative to the inhomogeneous line center. The two traces at the center were taken 6 min apart to show the repeatability of the statistical fine structure. In both the red and blue wings of the inhomogeneous line, single-molecule features are clearly observed. Laser intensity, 1.2 W/cm<sup>2</sup>.

Figure 1b,c shows high-resolution fluorescence excitation spectra over a 10 GHz spectral range taken with the fiber geometry. In case b, the laser polarization was selected so as to excite one eigenpolarization of the fiber which may be termed "vertical polarization" for convenience. Only a few strong structures are evident that might be identified as single molecules. However, when the incident laser polarization is rotated by 90° in order to excite the other eigenpolarization of the fiber ("horizontal" polarization, trace 1c), a large number of strong, narrow, repeatable single-molecule spectral features are observed. Therefore, the sample volume probed at the end of the fiber is apparently composed primarily of a single crystal in which the terrylene transition dipoles form an angle of about 15° with respect to the "horizontal" fiber axis (this orientation is fortuitous). In the following, the horizontal polarization of the incident laser will be used exclusively.

Figure 2 shows a selection of 10 GHz high-resolution fluorescence excitation spectra taken at different positions across the inhomogeneous line. The middle two traces, from the center of the band, are acquisitions of the same spectral region some minutes apart to show how highly repeatable the spectral structure is. This is the statistical fine structure<sup>27</sup> resulting from overlapping single-molecule peaks. To both the red and the blue of the inhomogeneous line center, well-defined, isolated single-molecule absorption lines are easily recorded. The background scattering signal from the polycrystalline hexadecane matrix is quite tolerable.

Figure 3, inset, shows a scan of a single-molecule feature at 572.197 nm with 0.2 W/cm<sup>2</sup> probing power to illustrate that the line shape is Lorentzian (smooth line) with low-power homogeneous line width  $\Delta\nu_H = 39 \pm 2 \text{ MHz}$  (FWHM). From the fluorescence emission lifetime, a lifetime-limited width of  $1/(2\pi T_1) = 42 \text{ MHz}$  would be expected. The observed line width

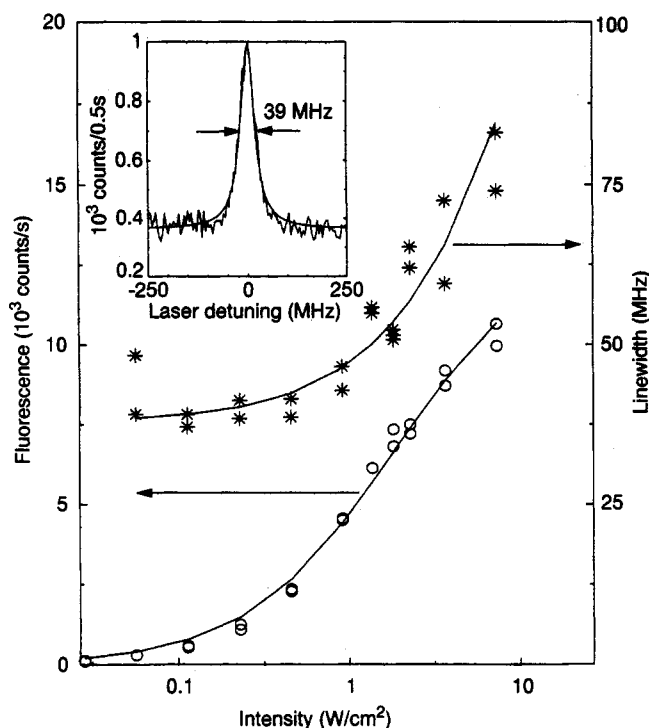


**Figure 3.** Saturation behavior and low-power line shape for a single molecule at 572.197 nm (molecule D in Table 1). Inset: the low-power line shape and a Lorentzian fit with FWHM 39 MHz. The stars represent line width measurements (right ordinate) and the open circles the peak rate measurements (left ordinate). The smooth curves are generated by fits to eqs 4 and 5 with fitting parameters of  $\Delta\nu_H = 39$  MHz,  $I_S = 1.91$  W/cm<sup>2</sup>, and  $R_\infty = 13\,000$  counts/s.

is in good agreement with this value, as would be expected from the generally crystalline local environment.

**Saturation Behavior.** Many single molecules showed no changes in resonance frequency for at least several minutes, and several such "stable" molecules were studied in a nonlinear incoherent saturation experiment. The line width  $\Delta\nu(I)$  (FWHM) and peak detected emission rate  $R(I)$  for one molecule at 572.197 nm were measured as a function of probing intensity to produce the data shown in the body of Figure 3. The solid curves represent nonlinear least-squares fits to the data using the standard expressions<sup>20</sup>

$$\Delta\nu(I) = \Delta\nu_H(1 + I/I_S)^{1/2} \quad (4)$$

and

$$R(I) = R_\infty(I/I_S)(1 + I/I_S)^{-1} \quad (5)$$

where  $I_S$  is the saturation intensity and  $R_\infty$  is the maximum (high power) emission rate. The single-molecule data are well-described by eqs 4 and 5 over 2.5 decades in intensity, with values for the fitting parameters of  $\Delta\nu_H = 39$  MHz,  $I_S = 1.91$  W/cm<sup>2</sup>, and  $R_\infty = 13\,000$  counts/s.

Data like those in Figure 3 were obtained for several single molecules on the red side of the inhomogeneous band to ascertain whether the saturation parameters show a distribution of values (see Table 1). Within experimental error, the low-power limiting line widths and peak emission rates do not vary from molecule to molecule. The  $I_S$  values, however, vary by as much as a factor of 2. It is important to recall that the intensity values quoted are calculated simply by dividing the power exiting the fiber by  $(3\,\mu\text{m})^2$ , which may not accurately reflect the absolute intensity pumping the molecule, especially if the transition dipole is not oriented exactly along the optical electric field. Furthermore, since the physical location of each molecule relative to the center of the core of the fiber (and hence relative to the center of the Gaussian beam emerging from the fiber) is unknown, such

**TABLE 1: Measured Low-Power Line Width  $\Delta\nu_H$  (Full Width at Half-Maximum), Saturation Intensity  $I_S$ , and (Detected) Saturation Count Rate  $R_\infty$  for Four Single Molecules of Terrylene in Hexadecane at 1.7 K Located at the Wavelengths Indicated**

molecule	$I_S$ (W/cm <sup>2</sup> )	$\Delta\nu_H \pm 2$ MHz	$R_\infty$ (counts/s)	$\lambda$ (nm)
A	1.28	40	12 000	573.902
B	0.89	41	10 000	572.000
C	1.47	40	11 400	571.996
D	1.91	39	13 000	572.197

apparent variations in saturation intensity cannot be regarded as significant.<sup>28</sup>

The much larger variations in  $I_S$  observed for pentacene in *p*-terphenyl<sup>3</sup> caused by differences in triplet photophysical parameters are apparently not occurring here, at least for the molecules investigated thus far. It appears that terrylene is much less sensitive than pentacene to steric effects that could bend the molecular framework and lead to changes in photophysical parameters.<sup>29</sup> In any case, the  $I_S$  values for terrylene are much larger than for pentacene, and the maximum emission rates are also larger, consistent with the previous work on terrylene in PE.<sup>13</sup> A more thorough analysis of the photophysical parameters for terrylene in hexadecane will be published separately.<sup>30</sup>

#### Images of Single Molecules by Fluorescence Microscopy.

Figure 4 shows a fluorescence microscopy image for a relatively stable single molecule of terrylene in hexadecane (molecule E) with 10 s accumulation time (analog mode, image rendered with IBM Data Explorer). The *x* and *y* axes correspond to the  $100\,\mu\text{m} \times 100\,\mu\text{m}$  spatial region imaged by the camera, and the *z* axis is the fluorescence signal. Since the laser frequency is chosen to resonate with only one molecule, a very strong peak appears on a moderate scattering background from the host matrix and from terrylene molecules not located in the focal plane of the microscope. The best evidence that the large peak is a single molecule is the fact that if the laser frequency is scanned over a range of approximately 100 MHz, the large single-molecule peak grows to a maximum and decays to the background. It is worth remarking that the fluorescence signal from the sample was so strong that it was possible to clearly see single molecules in each 40 ms frame acquired by the detector in real time (live, analog mode). Several hours of videotape were recorded of the behavior of selected single molecules as a function of laser excitation wavelength and time. Discontinuous changes in resonance frequency cause the bright spot in the image to completely disappear, and dynamical data taken directly from the videotape record will be described below.

**Resonance Frequency Changes—Dynamics of Single-Molecule Spectra.** Figure 5 shows a fascinating effect—time-dependent changes in resonance frequency of some single molecules, reminiscent of the resonance frequency changes reported earlier for pentacene in *p*-terphenyl and the polymer systems.<sup>1</sup> This behavior has a stochastic character, so the characteristics of the effect will be illustrated with several different single molecules in the remainder of this paper. Trace 5a, upper trace, shows a fluorescence excitation scan of two single molecules taken with the fiber setup. Close inspection of the first peak (inset) shows that the molecule apparently jumped out of resonance just as the laser frequency reached the peak of the line. A second scan of the same region (Figure 5a, lower trace) shows that the molecule had indeed disappeared from the laser scan range. Here, the time required to complete one laser scan was about 5 min, with a count time of 0.25 s at each of 1000 points.

A central question is whether or not such resonance frequency changes are either (i) spontaneous, and hence analogous to the spectral diffusion effects observed for single molecules of pentacene in *p*-terphenyl<sup>2</sup> and for the polymer systems, or (ii) light-driven, in which case the process is analogous to nonphotochemical hole-burning<sup>31</sup> observed in the polymer systems.<sup>10</sup> The rest of this

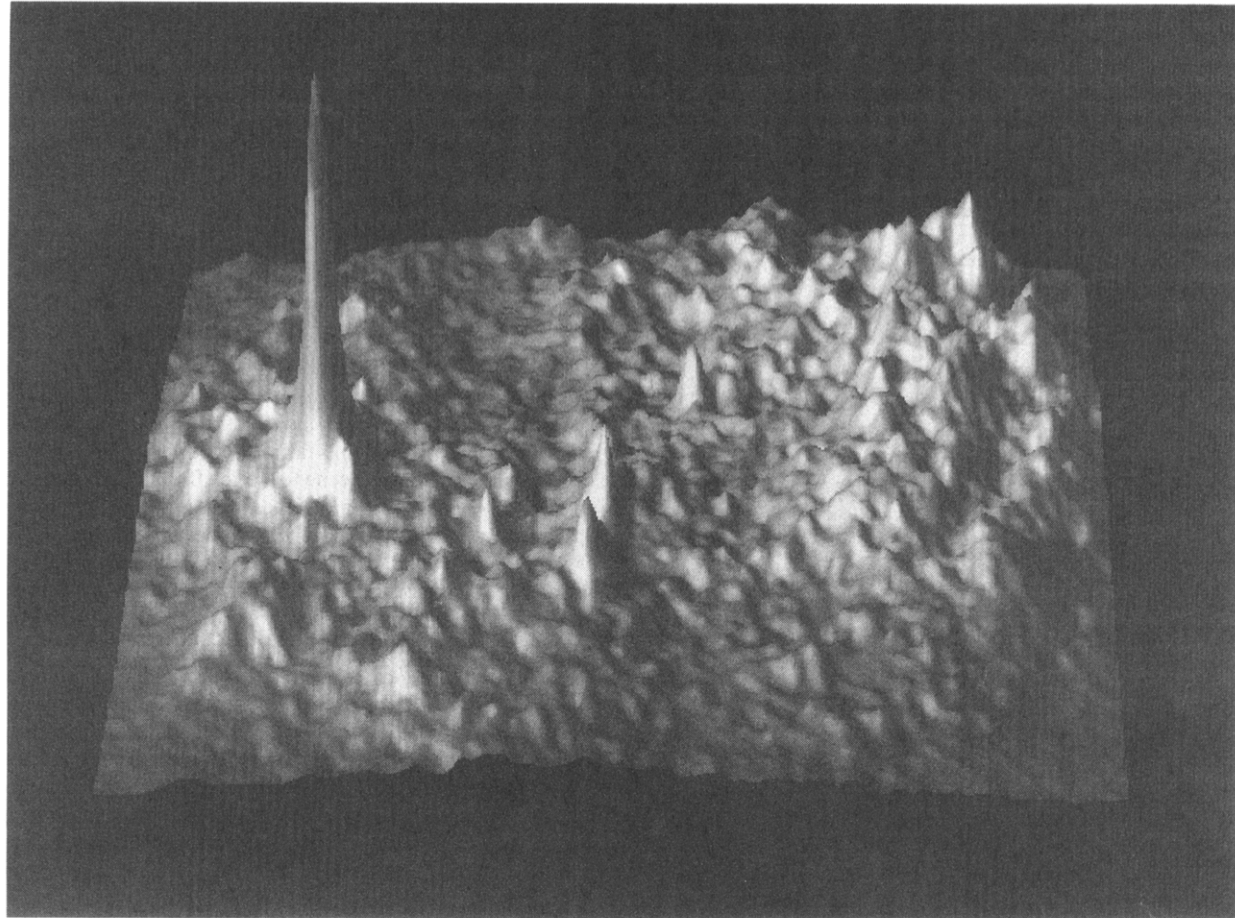


**Figure 4.** Fluorescence microscopy of a single molecule of terrylene in hexadecane (molecule E). The emission from a round sample of a diameter of  $100\ \mu\text{m}$  is shown with a fixed laser excitation wavelength of  $572.379\ \text{nm}$  with intensity  $20\ \text{mW}/\text{cm}^2$  and accumulation time  $10\ \text{s}$ . The integrated intensity under the peak is  $4700\ \text{photons}/\text{s}\cdot\text{molecule}$ , and each pixel is  $0.7 \times 0.5\ \mu\text{m}$ .

paper will provide evidence that most of the spectral changes we observe are light-driven. Previously, spectral diffusion processes in a Shpol'skii matrix were characterized by measurement of irreversible line broadening which occurs after thermal cycling of spectral holes.<sup>32</sup> This suggests that configurational changes are possible at low temperatures even in a locally crystalline Shpol'skii matrix.

Traces 5b and 5c illustrate the resonance frequency changes observed using the fiber setup for molecule D. In Figure 5b, the molecule was scanned 25 times in succession with a probing intensity of about  $1.7\ \text{W}/\text{cm}^2$ , and the spectral position of the single-molecule peak was recorded as a function of the time the spectrum was acquired. This trace is analogous to the trends or trajectories of single molecules of pentacene in *p*-terphenyl reported earlier,<sup>2</sup> although here the time resolution is much poorer ( $\approx 3\ \text{min}$  between observations instead of  $2.5\ \text{s}$ ). The molecule did not move by more than  $\pm 20\ \text{MHz}$  over a time period of  $1.5\ \text{h}$ . In fact, the observed changes in spectral position can easily be attributed to drift of the absolute laser frequency, as the manufacturer's specification is  $100\ \text{MHz}/\text{h}$  of drift. In this case, the laser was in resonance with the molecule for only about 7 s per scan.

Figure 5c shows much stronger irradiation of molecule D—the laser frequency was moved to the peak of the single-molecule excitation profile in the first few minutes, and the fluorescence emission was recorded as a function of time with probing intensity  $3.8\ \text{W}/\text{cm}^2$ . After approximately 3 min, the molecule jumped out of resonance, as evidenced by the sudden drop in fluorescence. After a dark period of about 8 min, the signal reappeared with full intensity, indicating that the resonance frequency returned to almost exactly the same value as before, similar to the case for perylene in PE.<sup>12</sup> This process happened again near 18 min and

reversed again near 25 min, after which no change occurred to the end of the observation time. These data suggest that a light-driven process is responsible for the resonance frequency changes because, at much higher probing fluence, spectral changes seem to occur more often.

Effects similar to those shown in Figure 5 were observed for several other single molecules: sometimes, a single molecule will disappear from resonance with the laser and return at a later time. Since the times in resonance and out of resonance are relatively long compared to the case for polymer systems,<sup>12,13</sup> care is required in attempting to make general conclusions.

**Two-State Molecules: A Light-Driven Molecular Switch.** On several occasions, single molecules with two resonance frequencies differing by  $\approx 140\ \text{MHz}$  were observed. Figure 6 illustrates this behavior using molecule F at  $572.206\ \text{nm}$  using both slow- and fast-scan excitation spectra taken with the lens/paraboloid setup. In the body of the figure, six sequential spectra are presented, each of which required  $40\ \text{s}$  to acquire, with times between acquisitions ranging from 2 to 10 min. Two well-defined resonance frequencies are apparent, and no other strong, in-focus single molecules were present in the  $2\ \text{GHz}$  scan range.

The inset to Figure 6 shows a gray-scale display of 2220 sequential scans taken with the fast-scan apparatus to examine molecule F in more detail. The horizontal axis is the laser frequency, and the vertical axis is the time the scan was recorded. The darkness of the image represents the size of the fluorescence emission signal. Two states are again clearly observed for molecule F, and the changes in resonance frequency are instantaneous on the time resolution of a single wavelength scan ( $2.56\ \text{s}$ ). Weaker, out-of-focus single molecules can also be observed, some of which are also showing resonance frequency shifts. Due to the relatively long time between resonance frequency changes, it was not easily



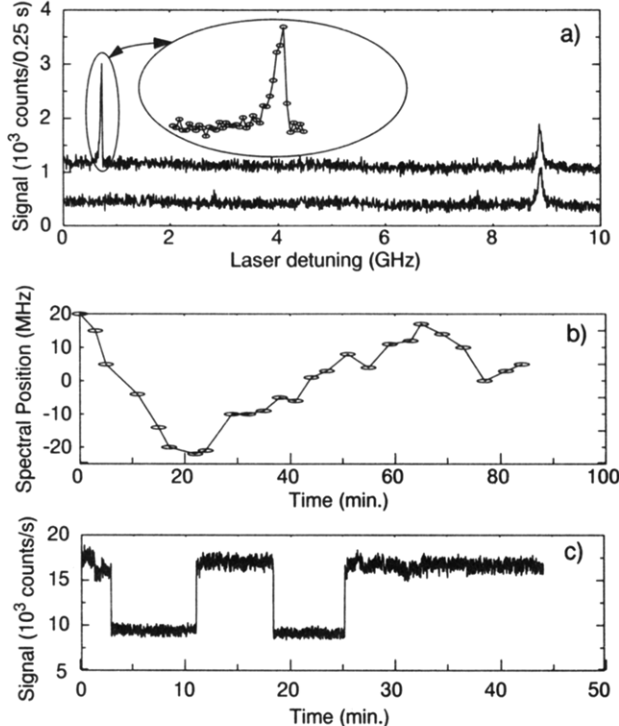


**Figure 5.** Resonance frequency changes for single molecules of terrylene in hexadecane. (a) Two scans of the same spectral region, showing the abrupt disappearance of the molecule highlighted in the inset. 0 GHz detuning corresponds to 571.490 nm. (b) Trend of center frequency for molecule D at 572.197 nm. Each symbol is derived from a single 2 min scan in which the scan rate was 7 s per line width. The solid line is a guide to the eye. (c) Time scan of the fluorescence emission from molecule D showing reversible changes in resonance frequency. The laser intensities are (b) 1.7 W/cm<sup>2</sup> and (c) 3.8 W/cm<sup>2</sup>.

possible to obtain convincing proof whether the process was affected by the laser intensity.

Such two-state behavior suggests that the terrylene optical transition is coupled to a single configurational degree of freedom

characterized by a double-well potential with two relevant energy states. This is the two-level system, or TLS model<sup>33</sup> used in many descriptions of amorphous system physics. Two-state behavior for a single molecule was observed earlier for perylene in PE<sup>12</sup> and for terrylene in PE,<sup>14,34</sup> but predominantly multistate behavior was observed for type II pentacene molecules in *p*-terphenyl.<sup>20</sup> The actual source for the TLS could be molecular reorientations of the nearby host matrix, or small reorientations of the impurity molecule itself with respect to the host.

Clear evidence that resonance frequency changes can be driven by the light was obtained for another molecule (G, at 572.370 nm) using the fluorescence microscopy setup. For many tens of minutes, every 40 ms image from the camera was recorded on videotape with fixed laser excitation wavelength. First, it was clearly observed for molecule G that whenever G disappeared from wavelength  $\lambda_1$ , the molecule could be easily found again (at the same spatial location) by displacing the laser frequency to lower values by  $\approx 155 \pm 10$  MHz to  $\lambda_2$ . This is in contrast to the reversible spectral hole-burning observed for perylene in PE in which the second resonance frequency was shifted away by more than  $\pm 2$  GHz.<sup>12</sup> Through the use of the 25 Hz frame rate as a clock, the time the molecule was in resonance and the time it was out of resonance could be easily determined by visual inspection of the videotape. We designate the molecule as being in “state 1” whenever the molecule emits brightly when the laser is at  $\lambda_1$ , and similarly for state 2.

Figure 7 shows the results of two such experiments for molecule G using 1.5 mW laser power. In the first experiment (open circles), the laser was held fixed at  $\lambda_1$  and the time in resonance (i.e., in state 1) and the time the molecule was off (“not 1”) were recorded. The average times marked with the arrows of  $\approx 60$  s are comparable at the power level used. It is a reasonable assumption (though not conclusively proven) that when the molecule is “not 1”, then it is actually in state 2. In the second experiment (filled squares), the laser was held fixed at  $\lambda_1$  as long as the molecule was in state 1, and then the laser was tuned to  $\lambda_2$  to measure how long the molecule stayed in state 2 with continuous pumping. In this case, the strong excitation by the laser significantly shortened the time in state 2 to an average time of  $\approx 2.9$  s. In a third experiment

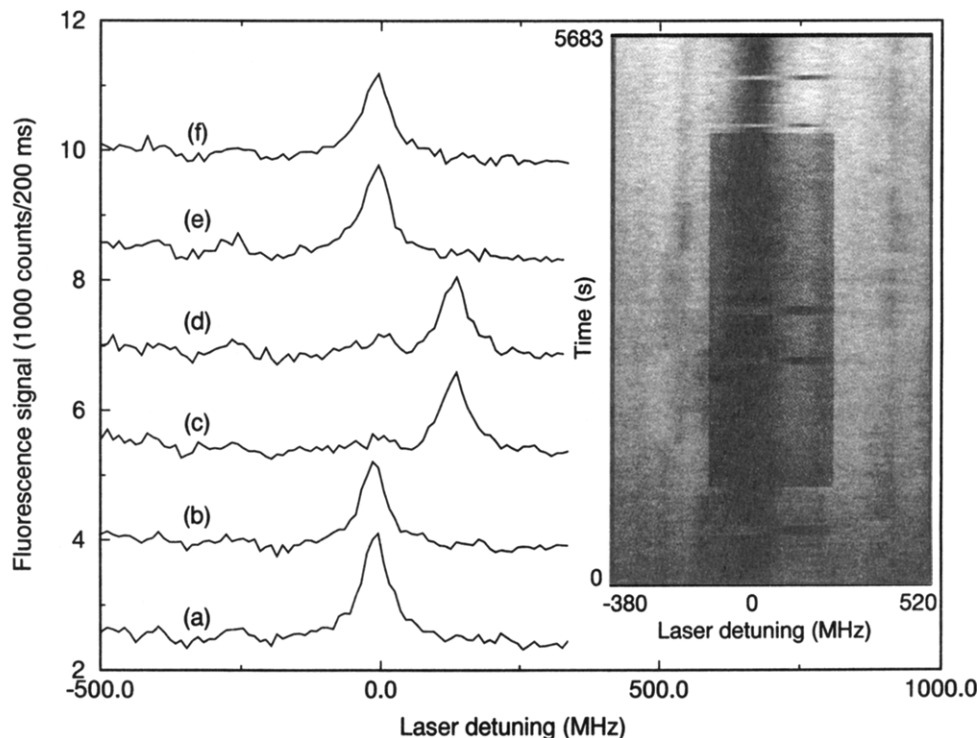


**Figure 6.** Resonance frequency changes for two-state molecule F at 572.206 nm using lens/paraboloid setup. (a–f): Six sequential fluorescence excitation spectra with 40 s per scan, 0.32 W/cm<sup>2</sup> laser intensity, and time between scans varying from 2 to 10 min. Inset: Gray-scale image of excitation spectra taken with fast-scan detection system, 10 ms/point, 256 points, 1.1 W/cm<sup>2</sup> probing intensity, and a total of 2220 scans over 5683 s.

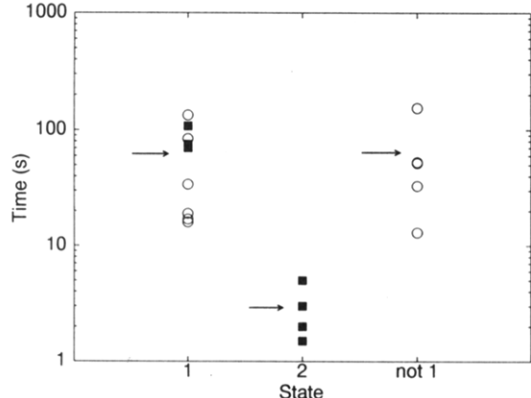


**Figure 7.** Kinetics of two-state molecule G at 572.370 nm measured with fluorescence imaging microscopy with laser power 1.5 mW. Times in resonance and out of resonance were measured using videotape images like that of Figure 4 with two different fixed laser frequencies as described in the text. Open circles: laser held fixed at  $\lambda_1$ . Filled squares: laser moved from  $\lambda$  to  $\lambda_2$  and back to follow the transitions between the two states. Arrows mark average times.

(not shown) at a lower laser power of 0.5 mW with the laser held fixed at  $\lambda_1$ , the average time in state 1 increased to 150 s. Interestingly, the average “not 1” time also increased to 160 s.

Taken together, these results provide evidence that the transformation from state 1 to state 2 is light-driven; thus the molecule with its nearby TLS can correctly be regarded as a light-controlled molecular switch. Further, it is clear that state 2 is less stable (more sensitive to light) than state 1. The increase in “not 1” time at the lower laser power suggests that when the laser is at  $\lambda_1$ , the  $2 \rightarrow 1$  transition might be driven by the laser pumping in the phonon side band of the optical absorption, as  $\lambda_1 < \lambda_2$ .

This fascinating behavior is clearly worthy of further study, since it raises several interesting possibilities as well as intriguing questions. It may be possible, for example, to determine which microscopic aspect of the local environment is responsible for the TLS itself. Such information could allow the elucidation of the microscopic mechanism for nonphotochemical hole-burning, a problem that has yet to be solved. Other interesting questions are the following: why is the spectral distance between the two states so small, and how does the light pumping the optical transition actually affect the TLS? It is reasonable that the optical effect on the TLS occurs either through excitation of internal vibrational modes of the molecule or by a local heating phenomenon produced by nonradiative decay. One would expect that the TLS coupled to the single molecule must be fairly close by in order to be able to be influenced by such local phonons. Yet a TLS so close to the molecule would be expected to produce a large spectral shift. It may be that the TLS is associated with a tiny change in a nearby *n*-alkane chain (such as a conformational change of the terminal methyl) which could have a small coupling to the nearby terrylene. Alternatively, it is possible that the TLS is associated with a slight reorientation of the terrylene with respect to the surrounding host (a librational tunneling effect). These two possibilities can be distinguished by performing experiments in perdeuterated hexadecane.

Finally, if any applications of this effect for optical storage on a single-molecule level<sup>35</sup> are to be considered practical, the kinetics of the light-driven transformation must be worked out in more detail and perhaps even modified to alter the efficiency, spectral spacing between the two states, and other properties.

In the two-state behavior observed for terrylene in PE,<sup>13,14</sup> a spectral distance between the two states of approximately several hundred megahertz was observed. The similarity between this shift and that for terrylene in hexadecane suggests a common origin and that perhaps the TLS responsible for the two-state behavior in PE is associated with the crystalline region rather

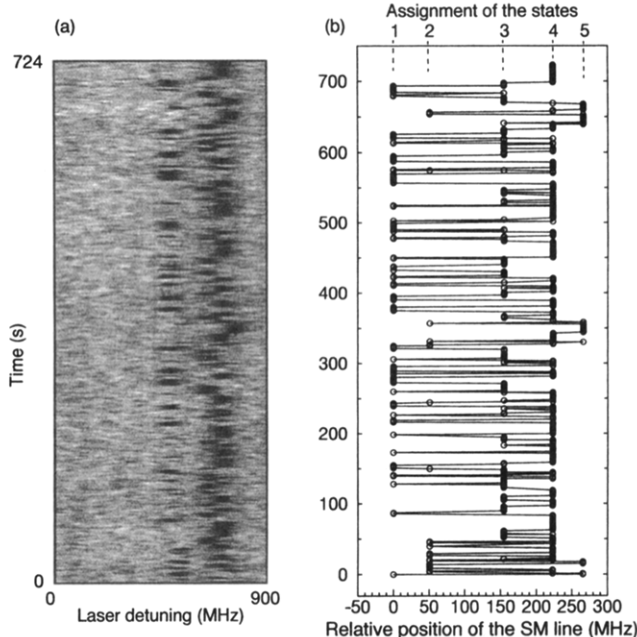


**Figure 8.** Multistate molecule H at 571.357 nm. (a) 566 scans of 256 points each, 5 ms per point plotted as a gray scale with vertical axis as time and horizontal axis as laser detuning. Laser intensity 0.36 W/cm<sup>2</sup>. (b) Time trajectory of the resonance frequency of (a) showing five states, with 0 MHz being the initial frequency. The lines are guides to the eye to show the time sequence.

than the amorphous region of the PE.<sup>36</sup> However, the TLS in the polymer was only rarely shown to be light-driven, and the change in rate was relatively small.<sup>34</sup>

**Dynamics of a Five-State Molecule.** Well-defined multistate behavior was also observed as shown in Figure 8 using the fast-scan acquisition system and the lens/paraboloid setup. Figure 8a shows a gray-scale display of 566 scans over 1000 MHz each of which took 1.28 s to acquire, with only 90% of the scan range shown. Black represents larger signals. By careful examination of the individual spectra, five distinct resonance frequencies can be observed. After the molecule is assigned to one of five possible resonance frequencies, a trajectory of the single molecule can be produced from the data as shown in Figure 8b. This behavior is similar to that reported earlier for pentacene in *p*-terphenyl,<sup>2</sup> and it suggests that the single molecule is coupled either to several TLS or to a multivalley configurational degree of freedom.

Again the issue of power dependence is crucial, and to test the influence of the probing laser, a trajectory like that in Figure 8 was acquired at 2 times lower laser power. As has been shown in a theoretical study of the pentacene in *p*-terphenyl system,<sup>37</sup> autocorrelation of measured trajectories is a useful first way to characterize the average time dependence. We note that, in contrast to direct measurements of the correlation at a fixed laser frequency,<sup>14</sup> here the time dependence of the full frequency trajectory is calculated. Figure 9 shows the autocorrelation of Figure 8b and a second autocorrelation from the lower-power data. At high power, the decay of the autocorrelation is well-described by a single exponential with time constant  $2.7 \pm 0.5$  s. At low power, the decay is biexponential with decay times  $1.9 \pm 1.1$  s and  $30 \pm 10$  s. It is clear that the increased probing laser power speeds up the dynamics of the system. Detailed conclusions beyond this will require data at more power levels and temperature dependence as well.

## Summary and Conclusion

In this work, the properties of a new material for SMS, terrylene in hexadecane, have been presented using slow laser scans, fluorescence microscopy images, and fast scans. Low-power line shapes and saturation data show that the lifetime-limited width



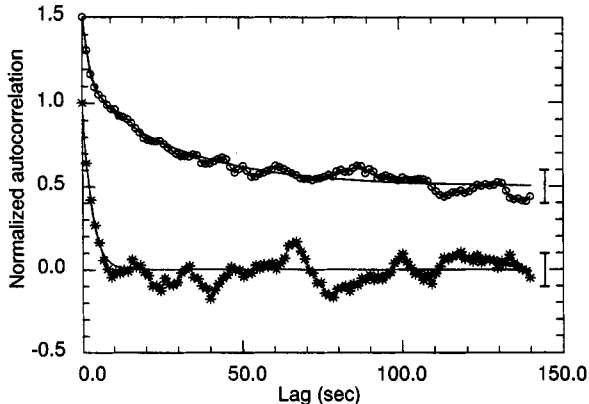


**Figure 9.** Autocorrelation of resonance frequency trajectory for molecule H at two power levels. Stars  $0.36 \text{ W/cm}^2$ , circles  $0.18 \text{ W/cm}^2$ , offset vertically for clarity. The lines are the functions  $[0.4 \exp(-t/1.9) + 0.6 \exp(-t/30)]$  (upper curve) and  $[\exp(-2.7)]$  (lower curve). The bars signify estimated error due to the finite length of the time trajectory.

is attained and that the saturation intensities and limiting emission rates are larger than for pentacene in *p*-terphenyl. Many single molecules are relatively stable compared to those in the polymer systems, which allows longer observation times and higher signal-to-noise.

A host of time-dependent changes in resonance frequency can be observed for specific single molecules, with both two-state and multistate behavior. Through variations of the laser power, evidence has been presented that these resonance frequency changes are laser-driven for several single molecules, so that the two-state case in particular can be regarded as a type of "molecular switch". Since a relatively long observation time is required to observe these changes, a thorough study of this effect must be the subject of future work. Nevertheless, terrylene molecules in hexadecane are clearly more stable than the earlier polymeric systems, but not as stable as the type I molecules for pentacene in *p*-terphenyl. The ordering of the local environment here provides much less inhomogeneity than that for the polymer systems, so it may be easier to construct theoretical models for the process.

Since the single-molecule spectra are strong, narrow, and relatively stable, this system can now be studied using many of the other tools of the optical spectroscopist, such as external field perturbations, photon correlation, and vibrational spectroscopy.<sup>23</sup> Since the host is a Shpol'skii matrix, it is reasonable to expect that this material is the first of a larger class of systems amenable to single-molecule spectroscopy. Through a study of the same probe molecule in a variety of host materials, detailed information about the nanoenvironment in the solid will be obtained.

**Acknowledgment.** We thank J. Keller for writing the real-time display program and M. Traber for the image data acquisition program. This work was supported in part by the Swiss National Science Foundation, ETH-Zürich, and IBM.

## References and Notes

- (1) For a review, see: Moerner, W. E.; Basché, Th. *Angew. Chem.* **1993**, *105*, 537; *Angew. Chem., Int. Ed. Engl.* **1993**, *32*, 457.
- (2) Ambrose, W. P.; Moerner, W. E. *Nature* **1991**, *349*, 225.
- (3) Bernard, J.; Fleury, L.; Talon, H.; Orrit, M. *J. Chem. Phys.* **1993**, *98*, 850.
- (4) Wild, U. P.; Güttler, F.; Pirotta, M.; Renn, A. *Chem. Phys. Lett.* **1992**, *193*, 451.
- (5) Croci, M.; Müschenborn, H.-J.; Güttler, F.; Renn, A.; Wild, U. P. *Chem. Phys. Lett.* **1993**, *212*, 71.
- (6) Basché, Th.; Moerner, W. E.; Orrit, M.; Talon, H. *Phys. Rev. Lett.* **1992**, *69*, 1516.
- (7) Güttler, F.; Sepiol, J.; Plakhotnik, T.; Mitterdorfer, A.; Renn, A.; Wild, U. P. *J. Lumin.* **1993**, *56*, 29.
- (8) Köhler, J.; Disselhorst, J. A. J. M.; Donckers, M. C. J. M.; Groenen, E. J. J.; Schmidt, J.; Moerner, W. E. *Nature* **1993**, *363*, 242.
- (9) Wrachtrup, J.; von Borczyskowski, C.; Bernard, J.; Orrit, M.; Brown, R. *Nature* **1993**, *363*, 244.
- (10) Basché, Th.; Moerner, W. E. *Nature* **1992**, *355*, 335.
- (11) Orrit, M.; Bernard, J.; Zumbusch, A.; Personov, R. I. *Chem. Phys. Lett.* **1992**, *196*, 595.
- (12) Basché, Th.; Ambrose, W. P.; Moerner, W. E. *J. Opt. Soc. Am. B* **1992**, *8*, 829.
- (13) Tchénio, P.; Myers, A. B.; Moerner, W. E. *J. Lumin.* **1993**, *56*, 1.
- (14) Zumbusch, A.; Fleury, L.; Brown, R.; Bernard, J.; Orrit, M. *Phys. Rev. Lett.* **1993**, *70*, 3584.
- (15) Moerner, W. E. *J. Lumin.*, in press.
- (16) Shpol'skii, E. V.; Il'ina, A. A.; Klimova, L. A. *Dokl. Acad. Nauk SSR* **1952**, *87*, 935. Shpol'skii, E. V. *Sov. Phys. Usp.* **1960**, *3*, 372. Shpol'skii, E. V. *Sov. Phys. Usp.* **1963**, *6*, 411.
- (17) See: Nakhimovsky, L.; Lamotte, M.; Joussot-Dubien, J. *Handbook of Low Temperature Electronic Spectra of Polycyclic Aromatic Hydrocarbons*; Elsevier: Amsterdam, 1989.
- (18) Plakhotnik, T.; Moerner, W. E.; Irngartinger, T.; Wild, U. P. *Chimia* **1994**, *48*, 31.
- (19) Clar, E. *Polycyclic Hydrocarbons*; Academic Press: London, 1964; Vol. 2, p 227.
- (20) Ambrose, W. P.; Basché, Th.; Moerner, W. E. *J. Chem. Phys.* **1991**, *95*, 7150.
- (21) Güttler, F.; Irngartinger, T.; Plakhotnik, T.; Renn, A.; Wild, U. P. *Chem. Phys. Lett.* **1994**, *217*, 393.
- (22) This was accomplished by fitting the various vibronic overtones to the usual expected Franck-Condon progression in order to determine the 0-0 fluorescence contribution, and the area under the phonon side band was taken to be negligible compared to the ZPL (see single-molecule vibrational spectra in ref 23).
- (23) Tchénio, P.; Myers, A. B.; Moerner, W. E. *Chem. Phys. Lett.* **1993**, *213*, 325.
- (24) This unpublished value was measured at 4.2 K by H. R. Gygas using time-correlated single-photon counting on a sample of terrylene in poly(ethylene) kindly provided by M. Orrit.
- (25) Norman, N.; Mathisne, H. *Acta Chem. Scand.* **1972**, *26*, 3913.
- (26) By summation of bond lengths from ref 19, Volume I, pp 119-125.
- (27) Moerner, W. E.; Carter, T. P. *Phys. Rev. Lett.* **1987**, *59*, 2705.
- (28) Under the assumption that the dipole moment, fluorescence yield, and excited state lifetimes are the same, the low-power slope of  $R(I)$  versus  $I$  should be the same for all molecules. In this case, the intensity axis can be rescaled so that the  $I_s$  values scale linearly with  $R_{\infty}$ . The resulting  $I_s$  values then vary over a 30% range, as do the  $R_{\infty}$  values.
- (29) Krysch, C.; Fleischhauer, H.-C.; Wagner, B. *Chem. Phys.* **1992**, *161*, 485.
- (30) Plakhotnik, T.; Moerner, W. E.; Palm, V.; Wild, U. P. In preparation.
- (31) Jankowiak, R.; Hayes, J. M.; Small, G. J. *Chem. Rev.* **1993**, *93*, 1471.
- (32) Zollfrank, J.; Friedrich, J. *J. Chem. Phys.* **1993**, *93*, 8586.
- (33) See: Phillips, W. A., Ed. *Amorphous Solids: Low-Temperature Properties*; Topics in Current Physics 24; Springer: Berlin, 1981.
- (34) Fleury, L.; Zumbusch, A.; Orrit, M.; Brown, R.; Bernard, J. *J. Lumin.* **1993**, *56*, 15.
- (35) Moerner, W. E. *Science*, in press.
- (36) Flory, P. J. *Pure Appl. Chem.* **1984**, *569*, 305.
- (37) Reilly, P. D.; Skinner, J. L. *Phys. Rev. Lett.* **1993**, *71*, 4257.